Acidic Amino Acids Impart Enhanced Ca^{2+} Permeability and Flux in Two Members of the ATP-gated P2X Receptor Family

Damien S.K. Samways and Terrance M. Egan

Department of Pharmacological and Physiological Science, Saint Louis University School of Medicine, St. Louis, MO 63104

P2X receptors are ATP-gated cation channels expressed in nerve, muscle, bone, glands, and the immune system. The seven family members display variable Ca^{2+} permeabilities that are amongst the highest of all ligand-gated channels (Egan and Khakh, 2004). We previously reported that polar residues regulate the Ca^{2+} permeability of the $P2X_2$ receptor (Migita et al., 2001). Here, we test the hypothesis that the formal charge of acidic amino acids underlies the higher fractional Ca^{2+} currents (*Pf*%) of the rat and human $P2X_1$ and $P2X_4$ subtypes. We used patch-clamp photometry to measure the *Pf*% of HEK-293 cells transiently expressing a range of wild-type and genetically altered receptors. Lowering the pH of the extracellular solution reduced the higher *Pf*% of the $P2X_1$ receptor but had no effect on the lower *Pf*% of the $P2X_2$ receptor, suggesting that ionized side chains regulate the Ca^{2+} flux of some family members. Removing the fixed negative charges found at the extracellular ends of the transmembrane domains also reduced the higher *Pf*% of $P2X_1$ and $P2X_4$ receptors, and introducing these charges at homologous positions increased the lower *Pf*% of the $P2X_2$ receptor. Taken together, the data suggest that COO^- side chains provide an electrostatic force that interacts with Ca^{2+} in the mouth of the pore. Surprisingly, the glutamate residue that is partly responsible for the higher *Pf*% of the $P2X_1$ and $P2X_4$ receptors is conserved in the $P2X_3$ receptor that has the lowest *Pf*% of all family members. We found that neutralizing an upstream His^{45} increased *Pf*% of the $P2X_3$ channel, suggesting that this positive charge masks the facilitation of Ca^{2+} flux by the neighboring Glu^{46}. The data support the hypothesis that formal charges near the extracellular ends of transmembrane domains contribute to the high Ca^{2+} permeability and flux of some P2X receptors.

The Journal of General Physiology

INTRODUCTION

A change in calcium concentration is an essential intracellular signal that initiates fundamental physiological processes such as secretion and contraction. To succeed in this role, the intracellular free Ca^{2+} concentration ($[Ca^{2+}]_i$) is tightly controlled, and nature has devised an impressive array of proteins that regulate Ca^{2+} transport across cell membranes (Berridge et al., 2003). Neurotransmitter receptors play an essential role in this process. Metabotropic receptors increase $[Ca^{2+}]_i$ by modulating voltage-gated Ca^{2+} channels or emptying internal Ca^{2+} stores (Ross et al., 2005). Ionotropic receptors, like the ATP-gated P2X receptor, take a more direct approach. P2X receptors are ligand-gated cation channels that increase $[Ca^{2+}]_i$ by forming a cation-permeable pore (Benham and Tsien, 1987). They are expressed in a diverse range of tissues and are particularly abundant in the nervous system (Khakh, 2001; Illes and Ribeiro, 2004; Khakh and North, 2006). Seven full-length subtypes ($P2X_{1-7}$) are expressed in mammals, and most are capable of forming both homo- and heteromeric receptors (Torres et al., 1999; North, 2002). The percentage of the ATP-gated current attributed to Ca^{2+} (*Pf*%) varies from ~3 to 15% depending on the subunit composition of the oligomeric receptor and the species of origin (Egan and Khakh, 2004). It is large enough to stimulate transmitter release from neurons (Pankratov et al., 2006), hormone release from endocrine glands (Troadec et al., 1998), and contraction of vascular smooth muscle (Ramme et al., 1987; Gitterman and Evans, 2001) and vas deferens (Brain et al., 2002).

Identifying the functional domains responsible for regulating Ca^{2+} flux is complicated by the lack of a clear picture of channel architecture. Each receptor is an oligomer of three subunits, with individual subunits comprised of intracellular amino and carboxy termini linked by two transmembrane domains and an extracellular loop (North, 2002). Mutagenesis studies indicate a role for the pore-lining second transmembrane segment (TM2) in the cation permeability (Migita et al., 2001) and Ca^{2+} current (Egan and Khakh, 2004) of at least one family member, the $P2X_2$ receptor. The first transmembrane segment (TM1) also lines the pore, and mutagenesis of this domain is known to alter permeability and gating (Samways et al., 2006).

We previously reported that ~6% of the total current through the $P2X_2$ receptor is carried by Ca^{2+} (Egan and Khakh, 2004), and that the ability of this receptor to select amongst cations involves a Ca^{2+}-sensing

Correspondence to Terrance Egan: egantm@slu.edu

Abbreviations used in this paper: BU, bead unit; HEK, human embryonic kidney; *Pf*%, fractional Ca^{2+} current; TM, transmembrane.

domain made of three polar amino acids of TM2 (Migita et al., 2001). This domain is absent in the two P2X receptors ($P2X_1$ and $P2X_4$) that display higher *Pf*%s of 11–15%, suggesting that distinct loci underlie the divergent Ca^{2+} currents of different family members. The aim of the present study was to identify the site(s) responsible for the elevated Ca^{2+} current of the $P2X_1$ and $P2X_4$ receptors.

MATERIALS AND METHODS

Molecular Biology and Cell Culture

We used wild-type rat $P2X_3$, human $P2X_4$ ($hP2X_4$), human $P2X_5$ ($hP2X_5$), and zebrafish $P2X_{4.1}$ ($zP2X_{4.1}$) receptors, and C-terminal epitope-tagged rat $P2X_1$ and $P2X_2$ receptors ($P2X_1$-EYMPME, $P2X_2$-DYKDDDDK) that were made and expressed using conventional techniques. Addition of epitope did not change the EC_{50} for ATP, the kinetics of the ATP-gated response (Torres et al., 1999), or, most importantly, the contribution of Ca^{2+} flux to total current through the channel pore of either parent receptor (Table I). Point mutations were introduced with the Quikchange II site-directed mutagenesis kit (Stratagene) and verified by automated DNA sequencing (Retrogen, Inc.). Chimerae were made as previously described (Haines et al., 2001a). All constructs were coexpressed with eGFP in human embryonic kidney-293 cells (HEK-293 or HEK-293T cells; American Type Culture Collection) using Effectene (QIAGEN) or Lipofectamine (Invitrogen) according to the manufacturers protocols. Transfected cells were maintained in Dulbecco's modified Eagle's medium (Invitrogen) supplemented with 10% FBS (Invitrogen or HyClone), 2 mM glutamine, 50 U/ml penicillin G, and 50 μg/ml streptomycin (Invitrogen), and incubated for 24–48 h at 37°C in a humidified, 5% CO_2 atmosphere. They were subsequently replated at low density onto poly-L-lysine–coated glass coverslips (Gold Seal; Becton Dickinson) the night before the experiment.

Patch-Clamp Photometry

Our use of the dye-overload method (Schneggenburger et al., 1993) is described in detail in Egan and Khakh (2004). In brief, we measured fractional calcium current (*Pf*%) by simultaneously measuring total membrane current and fluorescence in cells loaded with a high concentration (2 mM) of the calcium-sensitive dye, K_5fura-2 (for examples, see Fig. 2 A). Cells on coverslips were placed in a recording chamber mounted on the stage of a TE3000 epifluorescence microscope (Nikon Instruments). ATP-gated current was recorded from single cells held at −60 mV using borosilicate glass recording electrodes (1B150F, World Precision Instruments), an Axopatch 200B amplifier (Molecular Devices), ITC-16 data acquisition hardware (Instrutech), IGOR Pro software (Wavemetrics), and a G4 computer (Apple Computers). Electrodes had open-tip resistances of 1–3 MΩ and contained an intracellular solution of the following composition (in mM): 140 CsCl, 10 tetraethylammonium Cl, 10 HEPES, 2 K_5fura-2 (Molecular Probes/Invitrogen), 4.8 CsOH, pH 7.35. Light emitted from the 100-W xenon lamp was passed through a 380-nm bandpass filter and directed through the microscope objective (HMC 40X ELWD Plan Fluor; Modulation Optics, Inc.) into the recording chamber by reflection from the surface of a 400-nm dichroic long pass mirror. Light emitted by fura-2 was gathered by the objective, passed through the dichroic mirror and a 510-nm bandpass filter, and measured by a Model 714 Photomultiplier Detection System (Photo Technology International). We controlled the day-to-day variation in the sensitivity of the microscope/PMT by normalizing the fura-2 signal to a "bead unit" (BU). One BU equaled the average fluorescence of seven Carboxy Bright Blue 4.6-μm microspheres (Polysciences) measured one at a time on the morning of that day's experiment (Schneggenburger et al., 1993; Frings et al., 2000). Subsequent measurements of ATP-evoked changes in the fura-2 fluorescence of living cells were recorded as multiples of the daily BU. Cells were loaded with fura-2 by passive diffusion through the tip of the recording electrode. The time course of diffusion was measured in a subset of cells by monitoring the increase in intracellular fluorescence that results from fura-2 entry (Pusch and Neher, 1988). The time constant of loading was 144 ± 16 s ($n = 30$), and a near steady-state concentration of intracellular fura-2 was reached within ∼9–10 min of patch disruption. These measurements suggest that 10 min is the minimum time needed to equilibrate the intracellular compartment with the contents of the pipette, and we waited at least this long before acquiring data. The extracellular bath solution was (in mM) 140 NaCl, 2 $CaCl_2$, 1 $MgCl_2$, 10 glucose, and 10 HEPES, titrated to pH 7.4 with 4 NaOH. HEPES was replaced by MEPS in experiments performed at pH 5. ATP was applied for 0.2–2.0 s once every 2–3 min using triple-barreled theta glass and a Perfusion Fast-Step System SF-77 (Warner Instruments). For each construct and experimental algorithm, we used a concentration of ATP that evoked an easily measured decrease in fluorescence of fura-2 excited at 380 nm (ΔF_{380}) but avoided the problem of dye saturation (Table I). As previously reported, we saw no effect of short applications of submaximal concentrations of ATP on the fura-2 fluorescence of mock-transfected cells using the methods described above (Egan and Khakh, 2004).

The *Pf*% was calculated as follows:

$$Pf\% = \frac{Q_{Ca}}{Q_T} * 100.$$

Q_T is total charge and equal to the integral of the leak-subtracted ATP-gated transmembrane current. Q_{Ca} is the part of Q_T carried by Ca^{2+}, and is equal to ΔF_{380} divided by the calibration factor F_{max}. F_{max} was determined in a separate set of experiments as previously described (Egan and Khakh, 2004) and equaled 0.0185 ± 0.002 BU/nC ($n = 12$).

Ca^{2+} and Cl^- Permeability Measurements

We measured the relative permeabilities of Ca^{2+} and Cl^- to Cs^+ (P_{Ca}/P_{Cs} and P_{Cl}/P_{Cs}, respectively) using a reversal potential-based method and the Goldman equations (Hille, 2004). Membrane current was recorded using an AxoPatch 200B amplifier, indifferent electrodes suspended in 3 M KCl agar bridges in contact with the bath solution, and the broken-patch configuration of the whole-cell voltage-clamp technique. The solution in the recording pipette was (in mM) 150 CsCl, 10 EGTA, and 10 HEPES, brought to pH 7.4 with CsOH. Open tip electrode resistances measured 0.7–2.0 MΩ. Giga-ohm seals were established in a standard bath solution of (in mM) 150 NaCl, 1 $CaCl_2$, 1 $MgCl_2$, 10 glucose, and 10 HEPES, pH 7.4 with NaOH, and subsequently switched to test solutions of different ionic compositions.

To measure P_{Ca}/P_{Cs}, the bath solution was first changed to one that contained predominately CsCl (in mM: 150 CsCl, 0.1 $CaCl_2$, 1 $MgCl_2$, 10 glucose, 10 HEPES), followed by one that contained predominately Ca^{2+} (in mM: 112 $CaCl_2$, 1 $MgCl_2$, 10 glucose, 10 HEPES). We included 0.1 mM Ca^{2+} in the CsCl solution to retard pore dilation because this process causes a time-dependent change in cation permeability that could alter P_{Ca}/P_{Cs} (Khakh et al., 1999; Chaumont and Khakh, 2006); in theory, addition of 0.1 mM Ca^{2+} to a solution of 150 mM CsCl solution is expected to have a negligible effect on the reversal potential of ATP-gated current (Lewis, 1979). We changed the membrane voltage of

TABLE I

Pf% for Wild Type, Tagged, and Mutant $P2X_1$, $P2X_2$, $P2X_3$, and $P2X_4$ Receptors

	Protein	[ATP] (μM)	pA/pF	*Pf%*	*n*	Δ from $P2X_1$?	Δ from $P2X_2$?	Δ from $hP2X_4$?
$P2X_1$	WT $P2X_1$	3	77 ± 17	12.1 ± 0.8	8	–	Yes	Yes
	$P2X_1$-EE	3	152 ± 34	11.6 ± 0.6[a]	11	–	Yes	Yes
	(pooled $P2X_1$)	3	120 ± 20	11.8 ± 0.5	19	–	Yes	Yes
$P2X_2$	WT $P2X_2$	30	314 ± 22[b]	5.7 ± 0.4[c]	18	Yes	–	Yes
	$P2X_2$-FLAG	3	302 ± 41	6.7 ± 0.2[d]	55	Yes	–	Yes
Chimerae	$P2X_2$-$TM1_{X1}$	3	329 ± 66	9.3 ± 0.6	7	Yes	Yes	Yes
	$P2X_2$-$TM2_{X1}$	3	103 ± 23	2.6 ± 0.3	6	Yes	Yes	Yes
	$P2X_2$-$TM1/2_{X1}$	10	39 ± 16	8.9 ± 0.4	8	Yes	Yes	Yes
pH on WT	$P2X_1$ (pH 5)	10	111 ± 29	5.8 ± 0.8	6	Yes	No	Yes
	$P2X_2$ (pH 5)	3	257 ± 30	5.8 ± 0.8	6	Yes	No	Yes
$P2X_1$ mutants	$P2X_1$-E52Q	3	130 ± 20	8.4 ± 0.5	13	Yes	No	Yes
	$P2X_1$-E52Q (pH 5)	30	225 ± 65	6.0 ± 0.7[e]	9	Yes	No	Yes
	$P2X_1$-D327S	3	182 ± 35	10.5 ± 0.5	11	No	Yes	Yes
	$P2X_1$-DM	10	82 ± 20	6.1 ± 0.6[f]	11	Yes	No	Yes
	$P2X_1$-DM (pH 5)	30	39 ± 7	5.8 ± 1.6	6	Yes	No	Yes
	$P2X_1$-Y51H	3	90 ± 28	6.3 ± 0.8	6	Yes	No	Yes
	$P2X_1$-Y51V	3	85 ± 23	13.2 ± 1.3	6	No	Yes	No
$P2X_2$ mutants	$P2X_2$-Q52E	3	185 ± 57	11.2 ± 0.8	8	No	Yes	Yes
	$P2X_2$-S326D	3	140 ± 68	11.0 ± 0.9	5	No	Yes	Yes
	$P2X_2$-DM	10	107 ± 15	13.4 ± 0.9	12	No	Yes	No
	$P2X_2$-DM (pH 5)	3	132 ± 25	6.6 ± 1.3[g]	5	Yes	No	Yes
$P2X_3$	$P3X_3$	3	69 ± 21	4.8 ± 0.3	7	Yes	Yes	Yes
	$P2X_3$-H45Y	3	132 ± 39	6.7 ± 0.5[h]	6	Yes	No	Yes
$P2X_4$	$hP2X_4$	10	154 ± 53	16.0 ± 1.0	11	Yes	Yes	–
	$hP2X_4$-E51Q	10	101 ± 33	14.6 ± 1.1	7	No	Yes	No
	$hP2X_4$-D332S	10	199 ± 60	13.0 ± 0.6	7	No	Yes	No
	$hP2X_4$-DM	30	111 ± 22	8.6 ± 0.6[i]	8	Yes	No	Yes
	$zP2X_{4.1}$	1000	11 ± 3	7.3 ± 1.3	5	Yes	No	Yes

$P2X_1$-EE and $P2X_2$-FLAG are the epitope-tagged receptors ($P2X_1$-EYMPME and $P2X_2$-DYKDDDDK, respectively) that served as templates for mutagenesis. The concentrations of agonist ([ATP]) used in the study were chosen to give measurable responses while avoiding dye saturation, and the pA/pFs are the average current densities measured at these concentrations. Wild-type (WT) $P2X_1$ and epitope-tagged $P2X_1$-EE receptors did not differ in *Pf*%s, and the pooled data were used as control in subsequent statistical evaluations. Although the *Pf*% of the tagged $P2X_2$-FLAG receptor measured here is the same as that of the WT $P2X_2$ receptor measured in our previous work reported elsewhere (Egan and Khakh, 2004), we did not pool these two datasets because they were obtained in separate studies performed at distinct locations (Cambridge, UK versus St. Louis, MO). Thus, all comparisons in the present study reflect differences from the $P2X_2$-FLAG receptor. In the three rightmost columns, we compare the *Pf*%s of mutants and chimerae to the parent receptors. Data that are significantly different from $P2X_1$, $P2X_2$, and $hP2X_4$ receptors are marked "Yes" and data that show no difference are marked "No." All data were obtained at extracellular pH 7.4 except where noted.

[a]Not different from the WT $P2X_1$ receptor.

[b]Unpublished data ($n = 10$); Li, personal communication.

[c]Data ($n = 18$) from Egan and Khakh (2004).

[d]Not different from the WT $P2X_2$ receptor.

[e]Significantly different from $P2X_2$-E52Q (pH 7.4).

[f]Significantly different from WT $P2X_1$, $P2X_1$-E52Q, and $P2X_1$-S327S.

[g]Significantly different from $P2X_2$-DM (pH 7.4).

[h]Significantly different from the WT $P2X_3$.

[i]Significantly different from wild-type $hP2X_4$, $hP2X_4$-E51Q, and $hP2X_4$-S332S.

cells bathed in each solution from −80 to 60 mV at a constant rate (1.4 V/s) before and during applications of ATP, and measured the membrane voltage corresponding to the zero-current level (i.e., the E_{rev}) from the leak-subtracted currents. We calculated P_{Ca}/P_{Cs} as

$$\frac{P_{Ca}}{P_{Cs}} = \frac{\left(a_{Cs} * [Cs]_i\right) * \exp\left(\Delta E_{rev} * F/RT\right) * \left(1 + \exp\left(\Delta E_{rev} * F/RT\right)\right)}{4 * a_{Ca} * [Ca]_o},$$

where a_{Cs} and a_{Ca} are the activity coefficients of Cs^+ (0.75) and Ca^{2+} (0.25), respectively, ΔE_{rev} is $E_{rev,Ca} - E_{rev,Cs}$, T is temperature (295.15°K, equal to 22°C), and F and R are universal constants.

We used bath solutions containing different concentrations of CsCl to measure P_{Cl}/P_{Cs}. The first solution had the same concentrations (154 mM) of Cs^+ and Cl^- as the pipette solution. We applied a voltage ramp to obtain E_{rev} of the ATP-gated current and calculated the junctional offset as the deviation of the measured E_{rev} from the expected zero current level of 0 mV. This was then

subtracted from the E_{rev} obtained in a "low" CsCl bath solution that contained (in mM) 30 CsCl, 0.1 $CaCl_2$, 1 $MgCl_2$, 210 sucrose, 10 glucose, and 10 HEPES. P_{Cl}/P_{Cs} was calculated as

$$\frac{P_{Cl}}{P_{Cs}} = \frac{1 - \{[X]_i/[X]_o\} * \exp(\Delta E_{rev} * F/RT)}{\exp(\Delta E_{rev} * F/RT) - \{[X]_i/[X]_o\}},$$

where $[X]_i/[X]_o$ is the ratio of the intracellular and extracellular ion activities (Mitchell et al., 1997). Activity coefficients were determined by interpolation of the tabulated data of Robinson and Stokes (1970) and equaled 0.82 and 0.72 for 30 and 150 mM CsCl, respectively.

Data Analysis

All data are presented as the mean ± SEM for the number of experiments stated in the text. Significant differences amongst groups were determined using InStat (GraphPad Software) by one-way ANOVA with Tukey's post hoc, or Student's *t* test where appropriate. The P values of individual datasets are quoted in the text; values ≤0.05 were considered significant. We used the pooled data of wild-type $P2X_1$ and $P2X_1$-EE receptors as controls for comparisons to mutated receptors because we measured no difference in the *Pf*%s of these two groups (Table I).

RESULTS

The percentage of ATP current carried by Ca^{2+} varies significantly amongst members of the P2X receptor family. In the present study, we first focused on the $P2X_1$ and $P2X_2$ receptors because they transduce appreciably different Ca^{2+} fluxes. We measured *Pf*%s of 11.8 ± 0.5 and 6.7 ± 0.2% for the rat $P2X_1$ and $P2X_2$ receptors, respectively (Table I). These values are significantly different ($P < 0.001$) from each other and in good agreement with previously published results (Rogers and Dani, 1995; Egan and Khakh, 2004). With this baseline established, we examined the effect of genetic manipulation of channel structure on *Pf*% to gain insight into the molecular basis of the variability in Ca^{2+} flux throughout the P2X family.

To What Extent Do Individual Transmembrane Segments Influence Ca^{2+} Flux?

Empirical data suggest that both TM1 and TM2 line the ion-conducting pore of the $P2X_2$ receptor (Samways et al., 2006). Although no such data exist for the $P2X_1$ receptor, ATP activates cationic currents through chimeric $P2X_1/P2X_2$ proteins with swapped transmembrane domains (Werner et al., 1996; Haines et al., 2001a), and therefore it is reasonable to assume that the pores of both channels share a roughly similar design. If so, then the disparity in Ca^{2+} flux amongst receptors might reflect subtype-specific differences in the primary structures of their pore-lining domains. To determine the influence of individual segments, we investigated three chimeric channels in which one ($P2X_2$-$TM1_{x1}$ and $P2X_2$-$TM2_{x1}$) or both ($P2X_2$-$TM1/2_{x1}$) of the transmembrane segments of the $P2X_2$ channel were replaced by equivalent stretches of the $P2X_1$ channel (Fig. 1, A and B). All three chimerae formed functional channels when expressed in HEK-293 cells (Fig. 1 C).

We found that swapping transmembrane segments had quantifiable effects on *Pf*% (Fig. 2). The chimeric channel containing the first transmembrane segment of the $P2X_1$ channel in the $P2X_2$ background ($P2X_2$-$TM1_{X1}$) had a *Pf*% equal to 9.3 ± 0.6%, which was significantly greater ($P < 0.001$) than that of the wild-type $P2X_2$ channel. Substitution of both transmembrane segments ($P2X_2$-$TM1/2_{X1}$) had no greater effect (*Pf*% of 8.9 ± 0.5%) than replacing TM1 alone. In stark contrast, the chimeric $P2X_2$ channel containing the TM2 of $P2X_1$, ($P2X_2$-$TM2_{x1}$) exhibited a *Pf*% of 2.6 ± 0.3% that was significantly lower ($P < 0.001$) than both wild-type channels (Table I). These results suggest either that: (1) both transmembrane domains contribute to the regulation of Ca^{2+} current, each in their own way; or (2) construction of the chimerae produced nonspecific changes in the pore-forming domains that affect *Pf*%. To explore these possibilities, we used the less invasive methods described below.

The Ca^{2+} Flux of the $P2X_1$ Receptor Is pH Sensitive

The considerable Ca^{2+} fluxes of many ligand-gated channels result from an interaction with negatively charged acidic amino acids in the mouth of the pore (Keramidas et al., 2004; Jensen et al., 2005). We looked for an effect of ionized side chains by measuring the *Pf*% of $P2X_1$ and $P2X_2$ receptors at a lower pH where a greater proportion of the COO^- side chains would be protonated and hence neutral (Hille et al., 1975; Green and Andersen, 1991) (Fig. 3 A). The *Pf*% of the wild-type $P2X_1$ receptor at pH 5.0 was 5.8 ± 0.8%, a significant ($P < 0.001$) reduction when compared with that measured at pH 7.4. In contrast, the *Pf*% of the wild-type $P2X_2$ receptor was unaffected by changing pH (Fig. 3 D). These data suggest that the electrostatic attraction of Ca^{2+} by one or more acidic amino acids is responsible for the high *Pf*%s of the $P2X_1$ receptor, and that titratable carboxylates are unlikely to play a role in Ca^{2+} flux through the $P2X_2$ receptor.

Acidic Residues Regulate the Ca^{2+} Flux of the $P2X_1$ Receptor

Next, we used site-directed mutagenesis to locate the acidic amino acid(s) responsible for the high Ca^{2+} flux of the $P2X_1$ channel. The data obtained using chimeric receptors suggested that the search should first center on the transmembrane domains. We discounted the conserved aspartate of TM2 because it is present in all family members (bold black residues of Fig. 1 B), and instead looked for differences in the primary sequences of the transmembrane domains of channels that show higher ($P2X_1$, $P2X_4$) and lower ($P2X_2$) Ca^{2+} fluxes. $P2X_1$ and $hP2X_4$ channels have the highest *Pf*%*s* of all members of the extended family (Egan and Khakh, 2004). Both channels have acidic residues at homologous positions in TM1 (Glu^{52}-$P2X_1$ and Glu^{51}-$hP2X_4$) and TM2 (Asp^{327}-$P2X_1$ and Asp^{331}-$hP2X_4$) that are missing in the $P2X_2$ channel (bold red residues of Fig. 1 B).

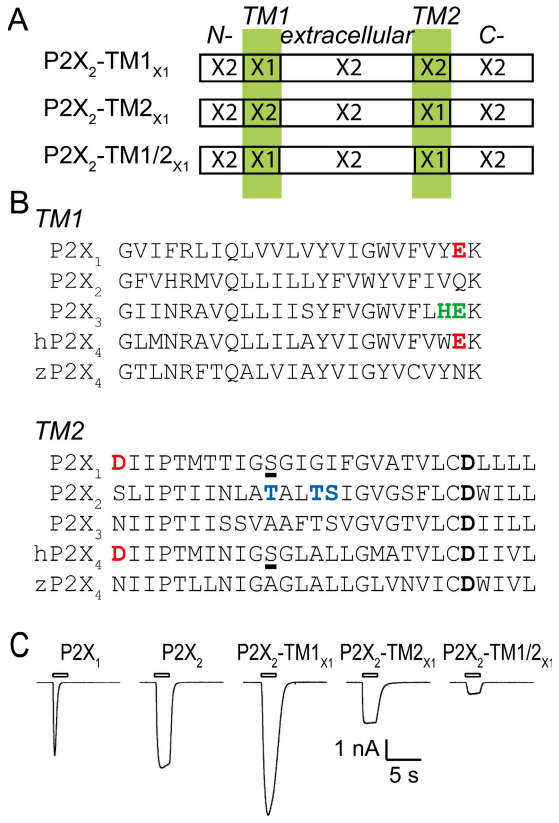

Figure 1. $P2X_2$ receptor chimerae. (A) Schematic representations of the receptor sequence for three $P2X_2$ chimerae. Native sections of the background $P2X_2$ receptor are labeled "X2" and sections substituted with corresponding parts of the $P2X_1$ receptor are labeled "X1." The chimerae contained amino acids Gly^{30}-Lys^{53} and/or Asp^{327}-Leu^{354} of the $P2X_1$ receptor. (B) Sequence alignments comparing the putative transmembrane segments of the $P2X_1$ (TM1, Gly^{30}-Lys^{53}; TM2, Asp^{327}-Leu^{354}), $P2X_2$ (TM1, Gly^{30}-Lys^{53}, TM2, Ser^{326}-Leu^{353}), $P2X_3$ (TM1, Gly^{24}-Lys^{47}; TM2, Asn^{317}-Leu^{344}), $hP2X_4$ (TM1, Gly^{29}-Lys^{52}; TM2, Asp^{331}-Leu^{358}), and $zP2X_4$ (TM1, Gly^{32}-Lys^{55}; TM2, Asn^{340}-Leu^{367}) receptors. The acidic amino acids that are the focus of this study (Glu^{52}-$P2X_1$, Glu^{51}-$P2X_4$, Asp^{327}-$P2X_1$, and Asp^{331}-$P2X_4$) are marked with bold red letters. The conserved aspartate (corresponding to $P2X_1$-Asp^{350}) found in all family members is marked with bold black letters. The polar residues of TM2 that regulate Ca^{2+} current through the $P2X_2$ receptor (Migita et al., 2001) are marked with bold blue letters. Note that a polar residue occupies only one of the three corresponding positions of the $P2X_1$ (Ser^{337}, underlined) and $hP2X_4$ (Ser^{350}, underlined) receptors. The neighboring amino acids (His^{45} and Glu^{46}) of the $P2X_3$ receptor are shown in bold green letters. (C) Currents recorded in the presence of ATP for the $P2X_1$, $P2X_2$, and the three chimeric receptors described in the text. ATP was applied for 2 s (open horizontal bars) at concentrations of 10 μM for the $P2X_2$-$TM1/2_{X1}$ chimera and 3 μM for the others.

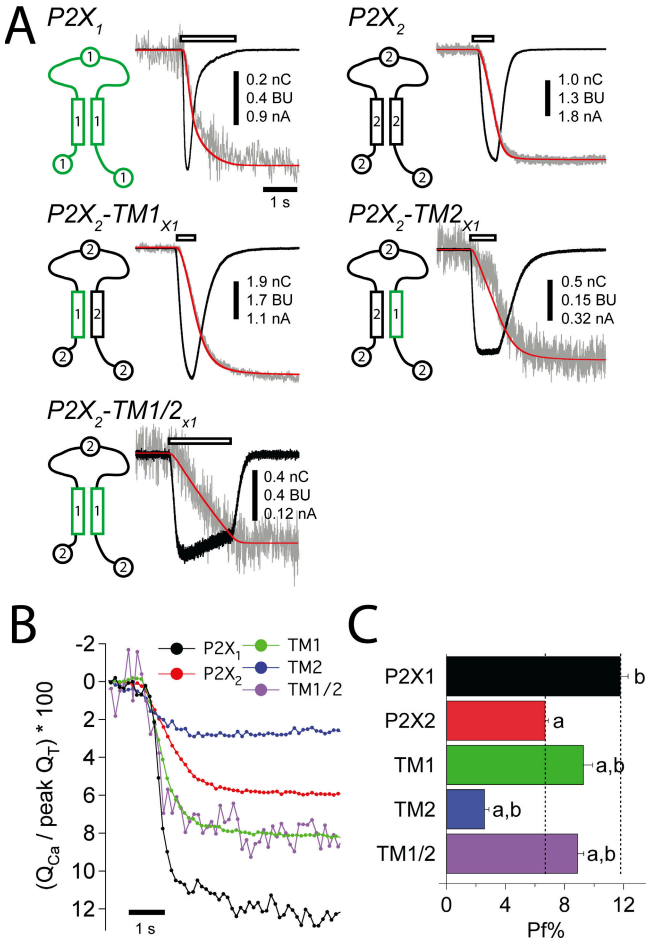

Figure 2. *Pf%* of chimerae. (A) Each panel shows a cartoon of the construct used to measure *Pf%*. The vertical open rectangles indicate transmembrane domains, and the sources of the different segments ($P2X_1$ or $P2X_2$) are marked with numbers. Next to the cartoons are current and fluorescence traces measured from cells expressing the indicated construct. The black traces are the ATP-evoked whole-cell currents (in amperes), the red traces are integrated current (in coulombs), and the gray traces are the change in F_{380} (in bead units). The duration of the ATP application is indicated by the horizontal open rectangles. (B) Here, and in Figs. 3 and 4, the sampling rate of the fluorescence signals are reduced by decimation to 10 Hz, converted to Q_{Ca} (where $Q_{Ca}=F_{380}/(F_{max}*BU)$), normalized to peak Q_T, and then multiplied by 100%. The amplitude of the steady-state value of each trace is equal to *Pf%*. (C) The bar graph shows the mean and standard error of the *Pf%* values. Values significantly different from the $P2X_1$ and $P2X_2$ receptors are marked with "a" and "b," respectively.

We engineered $P2X_1$ mutants in which one or both of these were replaced by the amino acids that occupy the equivalent positions in the $P2X_2$ receptor (Gln^{52} and Ser^{326}). Neutralizing fixed charge in TM1 ($P2X_1$-E52Q) significantly ($P < 0.001$) reduced *Pf%* to 8.4 ± 0.4% (Fig. 3 B and Table I). Removing the fixed charge in TM2 ($P2X_1$-D327S) had no significant effect (*Pf%* equals 10.5 ± 0.5%). However, neutralizing both charges ($P2X_1$-DM) caused a greater reduction (6.1 ± 0.6%) than neutralizing the charge of either TM1 ($P < 0.01$) or TM2 ($P < 0.001$) alone, and the sum of the effects of the single mutations (42% reduction in *Pf%*) was roughly equal to the effect of the double mutation alone (48% reduction in *Pf%*). Further, lowering the pH to 5.0 significantly ($P < 0.01$) reduced the *Pf%* of $P2X_1$-E52Q to 6.0 ± 0.7% but had no effect on $P2X_1$-DM (5.8 ± 1.6%), suggesting that the resident charge at

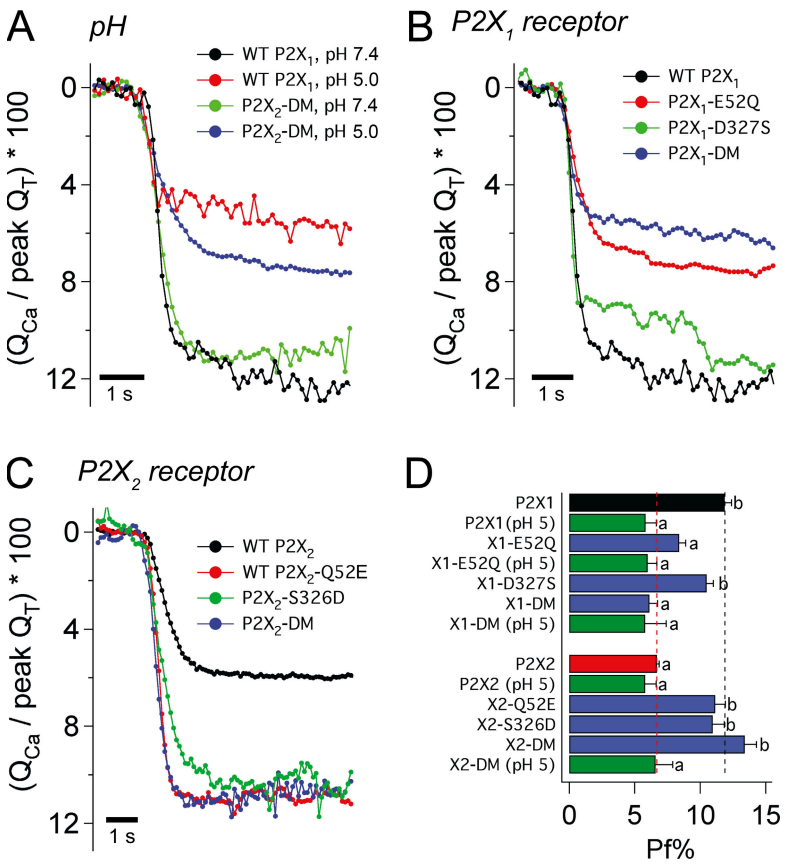

Figure 3. The role of acidic residues in regulating the Ca^{2+} flux of $P2X_1$ and $P2X_2$ receptors. Panel A shows representative traces recorded for $P2X_1$ and $P2X_2$-DM receptors at physiological (7.4) and acidic pH (5.0). Panel B shows the effects of removing the fixed charge of the $P2X_1$ receptor. Panel C shows the effects of adding fixed charge to the $P2X_2$ receptor. (D) The bar graph presents mean P*f*% data for all of the experiments. Values significantly different from the $P2X_1$ and $P2X_2$ receptors are marked with "a" and "b," respectively.

position 327 that is present in $P2X_1$-E52Q but missing in $P2X_1$-DM does affect *Pf*%. Taken together, these data argue that both Glu^{52} and Asp^{327} interact with Ca^{2+} in the mouth of the pore, although the relative contribution of each amino acid is different.

We also performed the converse experiment of placing carboxylates at appropriate sites in the $P2X_2$ receptor. We generated three mutant $P2X_2$ receptors in which one or both of Gln^{52} and Ser^{326} were replaced by glutamate or aspartate, respectively (Fig. 3, C and D). The *Pf*% for the single mutants $P2X_2$-Q52E and $P2X_2$-S326D were 11.2 ± 0.8 and 11.0 ± 0.9%, respectively. Both values are significantly greater ($P < 0.001$) than the wild-type $P2X_2$ receptor and approximately equal to the wild-type $P2X_1$ channel. Placing both mutations in a single construct ($P2X_2$-DM) did not increase *Pf*% more than either mutation alone. Lowering the pH to 5.0 significantly ($P < 0.001$) reduced the *Pf*% of $P2X_2$-DM to 6.6 ± 1.3%, (Fig. 3 A), suggesting that the increase in *Pf*% results from an electrostatic effect of the added charge and not an unintended change in protein structure.

The *Pf*% of the $P2X_4$ Receptor Decreases when Fixed Charge Is Removed

Next, we looked at the effects of mutagenesis on the $hP2X_4$ receptor because it shows the highest *Pf*% of all P2X receptors (Egan and Khakh, 2004) and, like the rat $P2X_1$ receptor, has fixed negative charge at the outer edges of its transmembrane segments. The *Pf*% of the wild-type hP2X4 receptor was 16.0 ± 1.0% (Fig. 4). We found that neutralizing both of the fixed charges of the transmembrane segments by mutagenesis gave a receptor ($hP2X_4$-DM) with a significantly ($P < 0.001$) reduced *Pf*% of 8.6 ± 0.6%. In contrast, removing a single charge had no effect. Specifically, the $hP2X_4$-E51Q and $hP2X_4$-D332S mutants had *Pf*%s of 14.6 ± 1.1 and 13.0 ± 0.6%, respectively, that were no different than the wild-type receptor. In this respect, the single charge deletion mutants of the $hP2X_4$ receptors resemble the single charge addition mutants of the $P2X_2$ receptor; the presence of one charge per subunit is enough to maintain a high Ca^{2+} flux through the pore.

As a final test, we measured the *Pf*% of the wild-type zebrafish $P2X_{4.1}$ receptor ($zP2X_{4.1}$) (Kucenas et al., 2003). It lacks the two relevant formal charges found in $hP2X_4$ receptors (Fig. 1 B) and therefore naturally replicates the charge reduction of $P2X_4$-DM. In keeping with our hypothesis, the *Pf*% of the $zP2X_{4.1}$ receptor at 7.3 ± 1.3% was significantly smaller than the $hP2X_4$ receptor and not different from the rat $P2X_2$ and $hP2X_4$-DM receptors (Fig. 4 B).

Neutralizing Fixed Charge Alters P_{Ca}/P_{Cs} but Not P_{Cl}/P_{Cs}

A caveat to using patch-clamp photometry to draw conclusions about the Ca^{2+} flux of cation channels is that it

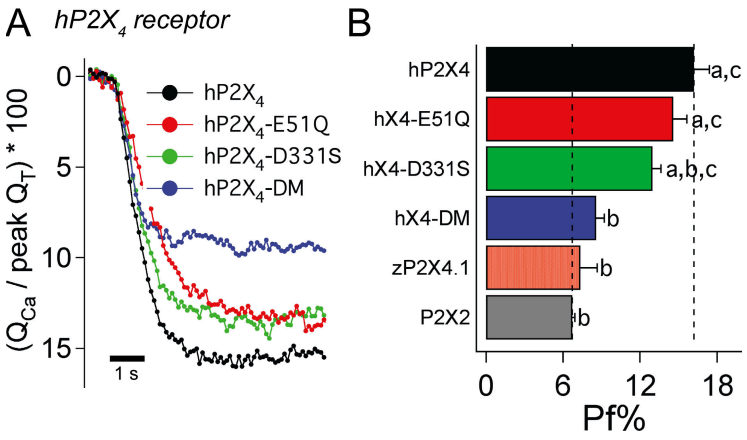

Figure 4. The role of acidic residues in regulating the Ca^{2+} flux of human and zebrafish $P2X_4$ receptors. Panel A shows representative traces recorded for single and double mutants of $hP2X_4$ receptors. Panel B presents mean *Pf*% data for all of the experiments. Values significantly different from the $P2X_2$, $hP2X_4$, and $hP2X_4$-DM receptors are marked with "a," "b," and "c," respectively.

does not account for the possibility that some mutations may render the channels anion permeable. With the exception of the human and chick $P2X_5$ receptors, most wild-type P2X receptors are cation selective and therefore impermeable to anion (Egan et al., 2006). However, it is possible that some mutations increase Cl^- permeability, and under the conditions of our experiments (equimolar [Cl^-] on either side of the membrane and a holding potential of −60 mV), such an effect would lead to an apparent inward current caused by efflux of Cl^-, a larger Q_T, and a reduction in *Pf*% that does not reflect a change in Ca^{2+} flux per se. To differentiate a change in Ca^{2+} permeability from a change in Cl^- permeability, we acquired reversal potential data from ATP-gated currents obtained from cells bathed in a range of extracellular solutions (see Materials and methods).

Switching the bath solution from one that contained 150 mM CsCl to one that contained 112 mM $CaCl_2$ caused a rightward shift in the reversal potential of the ATP-gated current of the wild-type $P2X_1$ and $hP2X_4$ receptors (Fig. 5 A) that translated to P_{Ca}/P_{Cs} values of 3.6 ± 0.2 and 4.6 ± 0.4, respectively (Table II). The shifts were smaller for $P2X_1$-DM and $hP2X_4$-DM receptors that lack the relevant formal charges, and the resulting P_{Ca}/P_{Cs}s were significantly ($P < 0.001$) lower than the wild-type templates at 2.6 ± 0.1 and 2.8 ± 01, respectively. They were not significantly different from that of the $P2X_2$ receptor that measured 2.9 ± 0.1 (Table II). Again, these data support our contention that formal charge influences the Ca^{2+} dynamics of $P2X_1$ and $P2X_4$ receptors.

In contrast, Cl^- permeability was not affected by the mutagenesis (Fig. 5 B). We first measured the P_{Cl}/P_{Cs} of the $hP2X_5$ receptor because it shows a significant Cl^- permeability (Bo et al., 2003). As expected, we found that switching to the 30 mM CsCl bath solution caused a ~6-mV shift in E_{rev}; the calculated P_{Cl}/P_{Cs} was 0.66 ± 0.12 (Fig. 5 B). We then measured the Cl^- permeability of wild-type and double mutant $P2X_1$ and $P2X_4$ receptors. Shifting the extracellular solution from one that contained 150 mM CsCl to one that contained 30 mM CsCl caused an approximately −30 mV shift in the ATP-gated current in all four constructs, demonstrating that both the wild-type and mutant receptors are largely impermeable to anions (Table II). These data support the hypothesis that the changes in *Pf*% that we measure after mutagenesis reflect specific effects on Ca^{2+} flux.

$P2X_3$ Has Fixed Charge but a Relatively Low *Pf*%

The glutamate of TM1 is conserved in only one other P2X subtype as Glu^{46} of the $P2X_3$ receptor. However, the $P2X_3$ receptor exhibits the lowest Ca^{2+} flux of all family members (Egan and Khakh, 2004). Unlike $P2X_1$ and $P2X_4$ receptors, the $P2X_3$ receptor contains a positively charged amino acid, His^{45}, immediately upstream to the conserved Glu^{46} residue (green residues of Fig. 1 B). His^{45} may provide a countercharge in the pore that serves to partially shield the neighboring Glu^{46} or simply repel Ca^{2+}, thus attenuating the ability of the carboxylate to attract Ca^{2+}. To test this hypothesis, we constructed a mutant $P2X_3$ receptor in which His^{45} was replaced by the tyrosine found at the homologous position of the $P2X_1$ receptor. This produced a small but significant ($P < 0.05$) increase in *Pf*% to 6.7 ± 0.5% compared with the wild-type $P2X_3$ control of 4.8 ± 0.3% (Table I).

We also generated mutant $P2X_1$ receptors in which Tyr^{51} was replaced by either a basic histidine ($P2X_1$-Y51H) or a neutral valine ($P2X_1$-Y51V). We found that the *Pf*% of $P2X_1$-Y51H was significantly reduced (6.3 ± 0.8%) compared with the wild-type $P2X_1$ receptor. This decrease was unlikely to be caused by a gross disruption of channel structure because substituting neutral valine (the corresponding residue of $P2X_2$) for Tyr^{51} had no effect on *Pf*% (Table I). Taken together, the data suggest that the identity of the amino acid just upstream of the conserved charges of $P2X_1$ and $P2X_3$ receptors helps to determine the magnitude of the Ca^{2+} flux through the channel pore.

DISCUSSION

We identified acidic residues at the outer ends of the transmembrane domains that contribute to the high

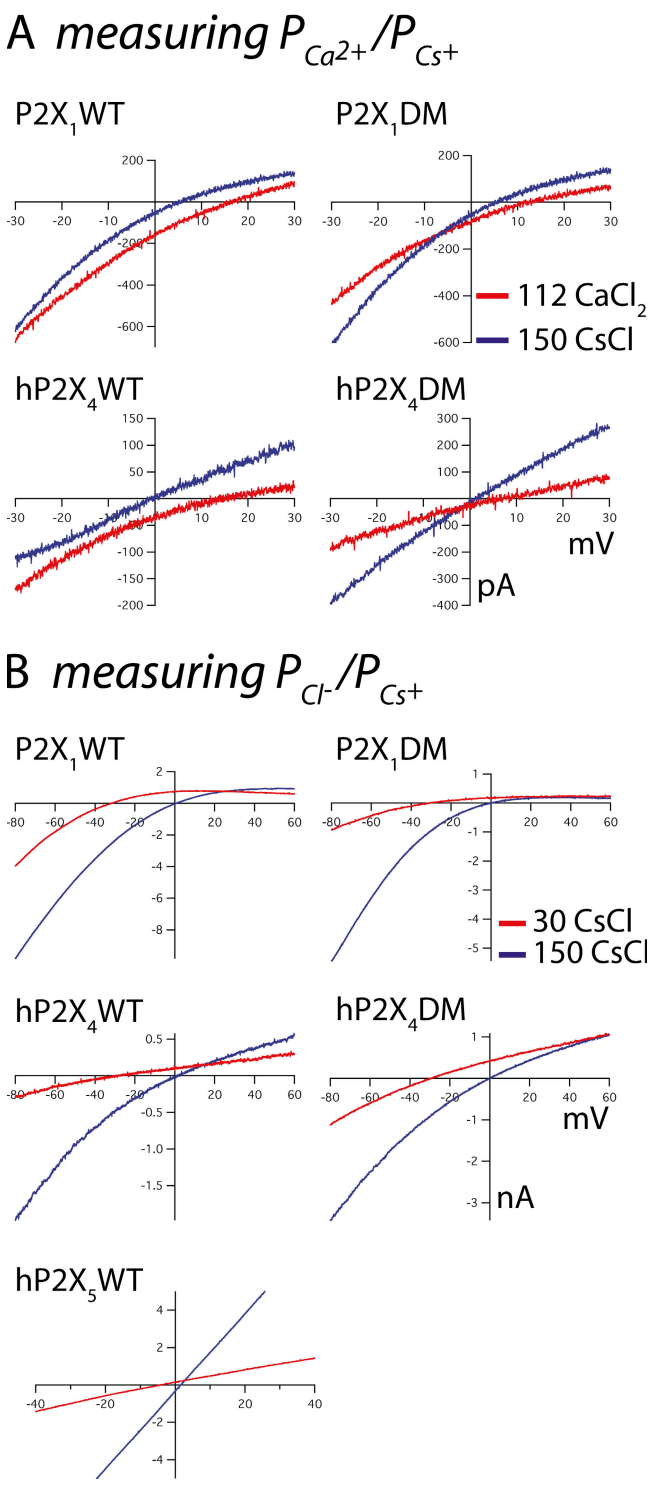

Figure 5. Voltage–current curves measured in different concentrations of extracellular Ca^{2+} or Cl^-. (A) The raw data traces show ATP-gated currents evoked in solutions that contained either Cs^+ (blue traces) or Ca^{2+} (red traces) as the dominant extracellular cation. The change in E_{rev} measured after switching from the Cs^+ to Ca^{2+} solution was smaller for the double mutant receptors (right traces) than it was for their wild-type templates (left traces), suggesting that eliminating formal charge decreased P_{Ca}/P_{Cs}. (B) The raw data traces show ATP-gated currents evoked in extracellular solutions that contained either 150 mM (blue traces) or 30 mM CsCl (red traces). For the wild-type $P2X_1$ and $hP2X_4$ receptors (top and middle left graphs), the change in E_{rev} measured upon switching to the low CsCl solution was ~30–33 mV as expected for a channel that showed a low Cl^- permeability. The same was true for the double mutant receptors that lacked the relevant formal charges of acidic amino acids (right traces), showing that mutagenesis did not change P_{Cl}/P_{Cs}. The change in E_{rev} was smaller in $hP2X_5$ receptors that show a significant Cl^- permeability (bottom left graph).

fractional Ca^{2+} current of ATP-gated $P2X_1$ and $P2X_4$ receptors. We found that acidification decreased the relatively large Ca^{2+} current of the $P2X_1$ receptor but had no effect on the smaller Ca^{2+} current of the $P2X_2$ receptor, suggesting that only the former uses acidic amino acids to discriminate amongst permeant cations. (We also looked at the effect of a lower pH on the $hP2X_4$ receptor. The concentration–response curve of the $P2X_4$ receptor shifts to the right at lower pHs, necessitating the use of a very high (>1 mM ATP) concentration of ATP to evoke a measurable ligand-gated current. At these high concentrations, applications of ATP evoked biphasic changes in intracellular calcium that did not follow the time course of the integrated current, making measurements of *Pf*% untenable.) The magnitude of the reduction is surprising when one considers the predicted degree of protonation of the COO^- side chains. We expected to measure a modest reduction in *Pf*% upon lowering the pH to 5.0, a value close to the pK_a of glutamate and aspartate in aqueous solution, and where half of the carboxyl groups are protonated and thus unable to attract Ca^{2+} (Falke et al., 1994). Instead, we found that acidification produced a *Pf*% equal to that of mutant receptors lacking both formal charges (i.e., $P2X_1$-DM). These data suggest that the pK_as of Glu^{52} and Asp^{327} of the $P2X_1$ receptor may be significantly higher than predicted from measurements of pure aqueous solutions of amino acids, an idea in keeping with published reports that the local microenvironment of a protein greatly influences the degree of ionization of its constituent amino acids (Fersht, 1985; Klockner et al., 1996; Seifert et al., 1999; Petsko and Ringe, 2004). Of particular interest is the positive charge provided by a conserved lysine (e.g., Lys^{53} of the $P2X_1$ receptor) that sits immediately downstream of Glu^{52}. Placing positive charge close to an acidic amino acid is enough to shift the latter's pK_a to 7.0 or higher (Falke et al., 1994). We have not pursued a study of this lysine because it is fully conserved and therefore unlikely to play a role in determining the dissimilar Ca^{2+} fluxes measured across the family. However, its role in the absolute magnitude of the Ca^{2+} flux should be considered in future experiments.

The idea that individual P2X receptors use distinct domains for cation selection is supported by the marked changes in *Pf*% observed in $P2X_1/P2X_2$ chimerae. Replacing the TM1 of the less Ca^{2+}-permeable $P2X_2$ receptor with that of the more permeable $P2X_1$ receptor

TABLE II

Relative Ca^{2+} and Cl^- Permeabilities Measured from Shifts in E_{rev}

Protein	$\Delta E_{rev,Ca}$	P_{Ca}/P_{Cs}	*n*	$\Delta E_{rev,Cl}$	P_{Cl}/P_{Cs}	*n*
$P2X_1$	9.3 ± 0.9	3.6 ± 0.2	6	−30.3 ± 1.1	0.09 ± 0.02	12
$P2X_1$-DM	3.9 ± 0.6	2.6 ± 0.1	5	−32.0 ± 1.2	0.07 ± 0.01	12
$P2X_2$	6.1 ± 0.4	2.9 ± 0.1	5		ND	
$hP2X_4$	12.6 ± 1.6	4.6 ± 0.4	7	−29.7 ± 1.4	0.09 ± 0.02	7
$hP2X_4$-DM	4.5 ± 1.0	2.8 ± 0.1	7	−32.9 ± 1.1	0.06 ± 0.02	7
$hP2X_5$		ND		−5.8 ± 2.5	0.66 ± 0.12	7

The control solution contained predominantly 150 mM CsCl, and the test solutions contained either 112 CaCl2 or 30 CsCl (see text for details). $\Delta E_{rev,Ca} = E_{rev,112\ Ca} - E_{rev,150\ CsCl}$. $\Delta E_{rev,Cs} = E_{rev,30\ CsCl} - E_{rev,150,CsCl}$.

significantly enhanced Ca^{2+} flux, as did addition of a single formal negative charge to the extracellular end of TM1 ($P2X_2$-Q52E). These data are important for three reasons: first, they add weight to the proposition that TM1 lines the outer segment of the ion channel (Haines et al., 2001b); second, they show for the first time that TM1 makes a measurable contribution to cation selection; and third, they suggest that the divergent Ca^{2+} currents of the $P2X_1$ and $P2X_2$ subtypes result in part from differences in the primary sequences of their TM1s.

The case of TM2 is more complex. We found that adding fixed negative charge to TM2 of the $P2X_2$ receptor increased *Pf*% only when Thr^{336}, Thr^{339}, and Ser^{340} are unperturbed (compare $P2X_2$-S326D to $P2X_2$-$TM2_{X1}$), a finding that supports previous reports that the polar residues of TM2 play an important role in Ca^{2+} flux in this receptor subtype (Egan and Khakh, 2004). Two of these are replaced by neutral amino acids in the $P2X_2$-$TM2_{X1}$ chimera, thus depriving the parent $P2X_2$ receptor of polar side chains that may provide the countercharge needed to partially dehydrate Ca^{2+} at a constriction within the pore (Migita et al., 2001). If so, then $P2X_1$ receptors either use other means to overcome the energy barrier provided by the constriction or lack it entirely. An alternative explanation is that the decrease in *Pf*% in the $P2X_2$-$TM2_{X1}$ chimera reflects nonspecific changes in the topology of the pore brought about by swapping one TM2 with another. This latter possibility is difficult to ignore, and additional experiments are needed to firmly establish a role for polar amino acids in ion permeation in some P2X receptors.

Many classes of ligand-gated cation channels use the formal charge of acidic amino acids positioned near the pore to facilitate Ca^{2+} transport into cells (Keramidas et al., 2004; Jensen et al., 2005). P2X receptors have three sites that could serve a similar function. One of these is fully conserved in TM2 (see bold black letters in Fig. 1 B) and therefore unlikely to explain the differences in Ca^{2+} flux measured here. Two nonconserved sites are present in $P2X_1$ and $P2X_4$ receptors but not in the $P2X_2$ receptor, and we found that removing both charges significantly decreased the *Pf*% and P_{Ca}/P_{Cs} without affecting P_{Cl}/P_{Cs}. Thus, our data are consistent with a model that uses the oxygen atoms of COO^- side chains to form an electrostatic ring that attracts cations. The attraction is stronger for Ca^{2+} than for Na^+, and therefore could explain the high Ca^{2+} permeability and flux of $P2X_1$ and $P2X_4$ receptors. The location of the ring in the permeation pathway is unknown because the inner and outer limits of the pore are poorly defined (Egan et al., 2006). We favor the hypothesis that it lies in the extracellular vestibule for the following two reasons. First, such a model is consistent with those that explain the high Ca^{2+} fluxes of other ligand-gated cation channels (Barry and Lynch, 2005). Second, models that incorporate the formal charges of aspartate and glutamate side chains into Ca^{2+} binding sites within the pore often result in channels that show Ca^{2+} block of monovalent current (Voets et al., 2004), and no such effect is reported for either the $P2X_1$ or $P2X_4$ receptors.

We suggest the simple hypothesis that the formal charges of both TM1 and TM2 influence the flux of Ca^{2+} through $P2X_1$ and $hP2X_4$ channels in a nonadditive fashion. We found that adding charge to either transmembrane domain significantly enhanced Ca^{2+} flux of the $P2X_2$ receptor, whereas removing the charge of either Glu^{51} or Asp^{332} had only a small effect on the *Pf*% of the $hP2X_4$ receptor. The results are therefore consistent, for together they suggest that (1) a single charge is sufficient to cause the elevated Ca^{2+} permeability noted in the $P2X_2$-DM and wild-type $hP2X_4$ receptors; and (2) there is very little summation in terms of increasing *Pf*% when both charges are present in the outer parts of TM1 and TM2.

For the $P2X_1$ receptor, it appears that Glu^{52} of TM1 might play a larger role than Asp^{327} of TM2. We found that removing Glu^{52} significantly reduced the *Pf*% of the $P2X_1$ receptor, whereas removing Asp^{327} had no effect, as might be expected if Asp^{327} is innocuous. Although these findings seem to invalidate the dual-charge hypothesis discussed above, two experiments suggest that Asp^{327} does influence Ca^{2+} flux through the channel. First, subtracting both charges (i.e., $P2X_1$-DM) has a significantly greater effect on the *Pf*% than removing

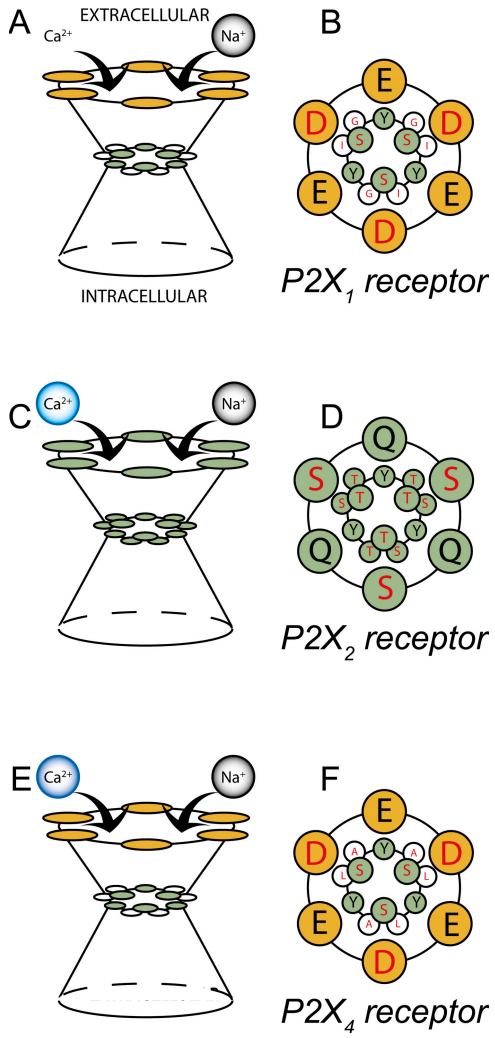

Figure 6. Schematic representations of the ion permeable pores of trimeric $P2X_1$, $P2X_2$, and $P2X_4$ receptors. Residues in TM1 are marked with black letters, and residues in TM2 are marked with red letters. The leftmost panels show side (A and E) and top (B and F) views of $P2X_1$ and $P2X_4$ receptors. The mouth of the pore is surrounded by an outer ring of six acidic amino acids (two from each of three subunits). The outer ring is missing in the $P2X_2$ receptor (C and D). Also shown are the three polar residues within TM2 of the $P2X_2$ receptor that are thought to form a polar ring at a narrow section of the channel pore. Only one of these sites is occupied by a polar amino acid in the $P2X_1$ and $P2X_4$ receptors. TM1 also contains a conserved tyrosine (Tyr^{43}) that may be properly positioned to contribute to the polar ring.

either Glu^{52} or Asp^{327} alone. Second, acidification decreases the *Pf*% of $P2X_1$-E52Q but has no effect on $P2X_1$-DM, and the only difference between these two mutants is the presence of Asp^{327}. It is difficult to explain why eliminating the glutamate of TM1 significantly decreases the *Pf*% of $P2X_1$ but not $P2X_4$ receptors, except to say that structural differences in TM2 may make the Asp^{327} of the $P2X_1$ receptor either less accessible to Ca^{2+} or less charged than either the Asp^{332} of the $hP2X_4$ receptor or the Asp^{326} of the $P2X_2$-S326D mutant. $P2X_1$, $P2X_2$, and $P2X_4$ receptors have remarkably different phenotypes and display unique agonist and antagonist profiles, rates of desensitization, Ca^{2+} permeabilities, and trafficking (North, 2002). If function follows structure, then structural differences between these subtypes are to be expected.

Fig. 6 shows cartoon representations of $P2X_1$, $P2X_2$ and $P2X_4$ receptors that incorporate two different models of Ca^{2+} transport. We assume that each channel is comprised of three subunits (Nicke et al., 1998; Aschrafi et al., 2004; Barrera et al., 2005; Mio et al., 2005), and that each subunit contributes two transmembrane segments to the pore (North, 2002). In $P2X_1$ and $P2X_4$ receptors, Ca^{2+} current is enhanced by a ring of charge made of glutamate and aspartate residues positioned in the outer mouth of the pore. These residues could function to accumulate extracellular Ca^{2+} in the permeation pathway by a simple electrostatic attraction, or form a binding site that selects Ca^{2+} over monovalent cations (Hille, 2004; Jensen et al., 2005). As mentioned above, the latter hypothesis seems doubtful because, unlike $P2X_2$ receptors, Ca^{2+} does not block monovalent cation current through $P2X_1$ receptors as expected for a binding site model (Evans et al., 1996). The extracellular ring of charge is missing in the $P2X_2$ receptor (Fig. 6, C and D). Instead, polar residues in the middle of the pore provide the countercharge needed to dehydrate Ca^{2+} in a narrow part of the pore (Migita et al., 2001). In this model, the narrow constriction provides an energy barrier that impedes current flow through the channel, and the relative conductance of cations is determined by their ability to momentarily "bind" to the polar side chains as they shed water. The presence of an intrapore binding site in $P2X_2$ receptors is supported by two findings. First, ATP-gated currents saturate with increasing concentrations of extracellular Na^+ (Ding and Sachs, 1999b). Second, monovalent current is blocked by low millimolar concentrations of extracellular Ca^{2+} (Nakazawa and Hess, 1993; Ding and Sachs, 1999a).

One question then remains: how well do these two mechanisms describe the Ca^{2+} current of other family members? Fixed charge is conserved in the highly Ca^{2+}-permeable $P2X_1$ and $P2X_4$ receptors, but is also present in the less permeable $P2X_3$ and $P2X_7$ receptors. We have not investigated $P2X_7$ receptors so far, but experiments with $P2X_3$ receptors suggest again that each subunit uses a slightly different method to select amongst cations. We suggest that the *Pf*% of the $P2X_3$ receptor is relatively low because of the presence of a unique His^{45} just upstream of Glu^{46}. The positive charge it supplies might serve to partially neutralize the negative charge of Glu^{46} and hinder the electrostatic interaction with Ca^{2+}. However, it is worth noting that neutralizing His^{45} did not elevate the *Pf*% of the $P2X_3$ receptor to a value equal to that of $P2X_1$ receptor, suggesting that additional factors contribute to the lower *Pf*% measured for $P2X_3$ receptor.

We gratefully acknowledge the help and guidance of Rosalie Uchanski, Mark Voigt, and Zhiyuan Li, the comments of Stephen Baylor, Baljit Singh Khakh, Keisuke Migita, and Florentina Soto, and the technical assistance of Angela Lipka and Steven Harris. The $hP2X_4$, $zP2X_{4.1}$, and $hP2X_5$ plasmids were gifts of Drs. Soto (University of Washington, Seattle, WA), Voigt (St. Louis University, St. Louis, MO), and R. Alan North (Manchester University, Manchester, UK), respectively.

This work was supported by the National Institutes of Health.

Olaf S. Andersen served as editor.

Submitted: 9 October 2006
Accepted: 6 February 2007

REFERENCES

Aschrafi, A., S. Sadtler, C. Niculescu, J. Rettinger, and G. Schmalzing. 2004. Trimeric architecture of homomeric $P2X_2$ and heteromeric $P2X1_{+2}$ receptor subtypes. *J. Mol. Biol.* 342:333–343.

Barrera, N.P., S.J. Ormond, R.M. Henderson, R.D. Murrell-Lagnado, and J.M. Edwardson. 2005. Atomic force microscopy imaging demonstrates that $P2X_2$ receptors are trimers but that $P2X_6$ receptor subunits do not oligomerize. *J. Biol. Chem.* 280:10759–10765.

Barry, P.H., and J.W. Lynch. 2005. Ligand-gated channels. *IEEE Trans. Nanobioscience.* 4:70–80.

Benham, C.D., and R.W. Tsien. 1987. A novel receptor-operated Ca^{2+}-permeable channel activated by ATP in smooth muscle. *Nature.* 328:275–278.

Berridge, M.J., M.D. Bootman, and H.L. Roderick. 2003. Calcium signalling: dynamics, homeostasis and remodelling. *Nat. Rev. Mol. Cell Biol.* 4:517–529.

Bo, X., L.H. Jiang, H.L. Wilson, M. Kim, G. Burnstock, A. Surprenant, and R.A. North. 2003. Pharmacological and biophysical properties of the human P2X5 receptor. *Mol. Pharmacol.* 63:1407–1416.

Brain, K.L., V.M. Jackson, S.J. Trout, and T.C. Cunnane. 2002. Intermittent ATP release from nerve terminals elicits focal smooth muscle Ca^{2+} transients in mouse vas deferens. *J. Physiol.* 541:849–862.

Chaumont, S., and B.S. Khakh. 2006. Regulation of ATP-gated P2X channel function by their cytosolic domains. *In* Biophysical Aspects of Ligand-gated Ion Channel Receptor Superfamilies. H. Arias, editor Research Signpost, NY. 445–460.

Ding, S., and F. Sachs. 1999a. Ion permeation and block of $P2X_2$ purinoceptors: single channel recordings. *J. Membr. Biol.* 172:215–223.

Ding, S., and F. Sachs. 1999b. Single channel properties of $P2X_2$ purinoceptors. *J. Gen. Physiol.* 113:695–720.

Egan, T.M., and B.S. Khakh. 2004. Contribution of calcium ions to P2X channel responses. *J. Neurosci.* 24:3413–3420.

Egan, T.M., D.S. Samways, and Z. Li. 2006. Biophysics of P2X receptors. *Pflugers Arch.* 452:501–512.

Evans, R.J., C. Lewis, C. Virginio, K. Lundstrom, G. Buell, A. Surprenant, and R.A. North. 1996. Ionic permeability of, and divalent cation effects on, two ATP-gated cation channels (P2X receptors) expressed in mammalian cells. *J. Physiol.* 497:413–422.

Falke, J.J., S.K. Drake, A.L. Hazard, and O.B. Peersen. 1994. Molecular tuning of ion binding to calcium signaling proteins. *Q. Rev. Biophys.* 27:219–290.

Fersht, A. 1985. Enzyme structure and mechanism. Second edition. W.H. Freeman, New York. 475 pp.

Frings, S., D.H. Hackos, C. Dzeja, T. Ohyama, V. Hagen, U.B. Kaupp, and J.I. Korenbrot. 2000. Determination of fractional calcium ion current in cyclic nucleotide-gated channels. *Methods Enzymol.* 315:797–817.

Gitterman, D.P., and R.J. Evans. 2001. Nerve evoked P2X receptor contractions of rat mesenteric arteries; dependence on vessel size and lack of role of L-type calcium channels and calcium induced calcium release. *Br. J. Pharmacol.* 132:1201–1208.

Green, W.N., and O.S. Andersen. 1991. Surface charges and ion channel function. *Annu. Rev. Physiol.* 53:341–359.

Haines, W.R., K. Migita, J.A. Cox, T.M. Egan, and M.M. Voigt. 2001a. The first transmembrane domain of the P2X receptor subunit participates in the agonist-induced gating of the channel. *J. Biol. Chem.* 276:32793–32798.

Haines, W.R., M.M. Voigt, K. Migita, G.E. Torres, and T.M. Egan. 2001b. On the contribution of the first transmembrane domain to whole-cell current through an ATP-gated ionotropic P2X receptor. *J. Neurosci.* 21:5885–5892.

Hille, B. 2004. Ionic Channels of Excitable Membranes. Volume 3. Sinauer Associates, Inc., Sunderland, MA. 814 pp.

Hille, B., A.M. Woodhull, and B.I. Shapiro. 1975. Negative surface charge near sodium channels of nerve: divalent ions, monovalent ions, and pH. *Philos. Trans. R. Soc. Lond. B Biol. Sci.* 270:301–318.

Illes, P., and J. Ribeiro. 2004. Molecular physiology of P2 receptors in the central nervous system. *Eur. J. Pharmacol.* 483:5–17.

Jensen, M.L., A. Schousboe, and P.K. Ahring. 2005. Charge selectivity of the Cys-loop family of ligand-gated ion channels. *J. Neurochem.* 92:217–225.

Keramidas, A., A.J. Moorhouse, P.R. Schofield, and P.H. Barry. 2004. Ligand-gated ion channels: mechanisms underlying ion selectivity. *Prog. Biophys. Mol. Biol.* 86:161–204.

Khakh, B.S. 2001. Molecular physiology of P2X receptors and ATP signalling at synapses. *Nat. Rev. Neurosci.* 2:165–174.

Khakh, B.S., X.R. Bao, C. Labarca, and H.A. Lester. 1999. Neuronal P2X transmitter-gated cation channels change their ion selectivity in seconds. *Nat. Neurosci.* 2:322–330.

Khakh, B.S., and R.A. North. 2006. P2X receptors as cell-surface ATP sensors in health and disease. *Nature.* 442:527–532.

Klockner, U., G. Mikala, A. Schwartz, and G. Varadi. 1996. Molecular studies of the asymmetric pore structure of the human cardiac voltage-dependent Ca^{2+} channel. Conserved residue, Glu-1086, regulates proton-dependent ion permeation. *J. Biol. Chem.* 271:22293–22296.

Kucenas, S., Z. Li, J.A. Cox, T.M. Egan, and M.M. Voigt. 2003. Molecular characterization of the zebrafish P2X receptor subunit gene family. *Neuroscience.* 121:935–945.

Lewis, C.A. 1979. Ion-concentration dependence of the reversal potential and the single channel conductance of ion channels at the frog neuromuscular junction. *J. Physiol.* 286:417–445.

Migita, K., W.R. Haines, M.M. Voigt, and T.M. Egan. 2001. Polar residues of the second transmembrane domain influence cation permeability of the ATP-gated $P2X_2$ receptor. *J. Biol. Chem.* 276:30934–30941.

Mio, K., Y. Kubo, T. Ogura, T. Yamamoto, and C. Sato. 2005. Visualization of the trimeric $P2X_2$ receptor with a crown-capped extracellular domain. *Biochem. Biophys. Res. Commun.* 337:998–1005.

Mitchell, C.H., L. Wang, and T.J. Jacob. 1997. A large-conductance chloride channel in pigmented ciliary epithelial cells activated by GTPγS. *J. Membr. Biol.* 158:167–175.

Nakazawa, K., and P. Hess. 1993. Block by calcium of ATP-activated channels in pheochromocytoma cells. *J. Gen. Physiol.* 101:377–392.

Nicke, A., H.G. Baumert, J. Rettinger, A. Eichele, G. Lambrecht, E. Mutschler, and G. Schmalzing. 1998. $P2X_1$ and $P2X_3$ receptors form stable trimers: a novel structural motif of ligand-gated ion channels. *EMBO J.* 17:3016–3028.

North, R.A. 2002. Molecular physiology of P2X receptors. *Physiol. Rev.* 82:1013–1067.

Pankratov, Y., U. Lalo, A. Verkhratsky, and R.A. North. 2006. Vesicular release of ATP at central synapses. *Pflugers Arch.* 452:589–597.

Petsko, G.A., and D. Ringe. 2004. Protein Structure and Function. New Science Press Ltd., London. 195 pp.

Pusch, M., and E. Neher. 1988. Rates of diffusional exchange between small cells and a measuring patch pipette. *Pflugers Arch.* 411:204–211.

Ramme, D., J.T. Regenold, K. Starke, R. Busse, and P. Illes. 1987. Identification of the neuroeffector transmitter in jejunal branches of the rabbit mesenteric artery. *Naunyn Schmiedebergs Arch. Pharmacol.* 336:267–273.

Robinson, R.A., and R.H. Stokes. 1970. Electrolyte Solutions. Second edition. Butterworths, London. 571 pp.

Rogers, M., and J.A. Dani. 1995. Comparison of quantitative calcium flux through NMDA, ATP, and ACh receptor channels. *Biophys. J.* 68:501–506.

Ross, W.N., T. Nakamura, S. Watanabe, M. Larkum, and N. Lasser-Ross. 2005. Synaptically activated Ca^{2+} release from internal stores in CNS neurons. *Cell. Mol. Neurobiol.* 25:283–295.

Samways, D.S., Z. Li, and T.M. Egan. 2006. Binding, gating, and conduction of ATP-gated ion channels. *In* Biophysical Aspects of Ligand-gated Ion Channel Receptor Superfamilies. H. Arias, editor. Research Signpost, NY. 419–443.

Schneggenburger, R., Z. Zhou, A. Konnerth, and E. Neher. 1993. Fractional contribution of calcium to the cation current through glutamate receptor channels. *Neuron.* 11:133–143.

Seifert, R., E. Eismann, J. Ludwig, A. Baumann, and U.B. Kaupp. 1999. Molecular determinants of a Ca^{2+}-binding site in the pore of cyclic nucleotide-gated channels: S5/S6 segments control affinity of intrapore glutamates. *EMBO J.* 18:119–130.

Torres, G.E., T.M. Egan, and M.M. Voigt. 1999. Hetero-oligomeric assembly of P2X receptor subunits. Specificities exist with regard to possible partners. *J. Biol. Chem.* 274:6653–6659.

Troadec, J.D., S. Thirion, G. Nicaise, J.R. Lemos, and G. Dayanithi. 1998. ATP-evoked increases in $[Ca^{2+}]$i and peptide release from rat isolated neurohypophysial terminals via a P2X2 purinoceptor. *J. Physiol.* 511:89–103.

Voets, T., A. Janssens, G. Droogmans, and B. Nilius. 2004. Outer pore architecture of a Ca^{2+}-selective TRP channel. *J. Biol. Chem.* 279:15223–15230.

Werner, P., E.P. Seward, G.N. Buell, and R.A. North. 1996. Domains of P2X receptors involved in desensitization. *Proc. Natl. Acad. Sci. USA.* 93:15485–15490.